

PSFC/JA-97-6

**LOWER BOUND IN ENERGY
FOR CHAOTIC DYNAMICS OF IONS**

D. Benisti, A. K. Ram, and A. Bers

April 1997

Plasma Science and Fusion Center
Massachusetts Institute of Technology
Cambridge, Massachusetts 02139 USA

This work was supported in part by a Lavoisier grant from the French Ministère des Affaires Etrangères; by DOE Grant No. DE-FG02-91ER-54109; and by NSF Grant No. ATM-94-24282. Reproduction, translation, publication, use and disposal, in whole or part, by or for the United States Government is permitted.

To be published in *Physics Letters A*.

**LOWER BOUND IN ENERGY
FOR CHAOTIC DYNAMICS OF IONS**

D. Benisti, A. K. Ram, and A. Bers

TABLE OF CONTENTS

Abstract	1
Text	2
Acknowledgements	15
References	16
Figure Captions	18
Figures	20

Lower Bound in Energy for Chaotic Dynamics of Ions

D. Bénisti, A. K. Ram, and A. Bers

Plasma Science and Fusion Center, Massachusetts Institute of Technology,

Cambridge MA 02139

Abstract: When a charged particle is acted upon by an electrostatic wave propagating across a uniform magnetic field, its dynamics is chaotic provided that its initial Larmor radius is larger than a threshold value ρ_m . We analytically compute ρ_m when the wave frequency is an integer multiple of the particle cyclotron frequency, and show that ρ_m increases with the wave amplitude. This leads to the counter-intuitive result that the dynamics of a low energy particle can be made stochastic by decreasing the amplitude of the wave.

Keywords: Hamiltonian dynamics, plasma physics, chaos, web structure, perturbation theory, Lie transform.

The motion of an ion in an electrostatic wave propagating perpendicularly to a uniform magnetic field has been studied extensively¹⁻⁷, due to its relevance in various areas of plasma physics such as tokamak heating⁸, or space plasma physics⁹. The energization of ions by a single wave in a uniform magnetic field occurs when the ions' dynamics are chaotic. One distinguishes two cases in such single wave-particle interactions: "off-resonance", $\omega \neq n\Omega$, i.e., where the wave frequency ω is not an exact integer multiple of the particle's cyclotron frequency Ω ; and "on-resonance" where $\omega = n\Omega$. In the off-resonance case, it has been shown in Ref. 1 that, above a threshold wave amplitude, chaotic dynamics occur only above a certain minimum value of the particle's energy; this minimum energy *decreases* slowly with increasing wave amplitude. In the on-resonance case, the particle's phase space is characterized by a web structure which is chaotic even at small wave amplitudes⁵. We show here that the stochastic web phase space also has a lower bound below which the particle's dynamics is regular. In contrast with the off-resonance case, we show that this lower bound *increases* with wave amplitude. Thus, while the web phase space becomes more stochastic with increasing wave amplitude, increasing the wave amplitude also increases the required initial energy a particle must have in order to access the chaotic web

for energization. Or, conversely, low energy particles can be made to access the chaotic web by lowering the wave amplitude.

The motion of a charged particle in a uniform magnetic field $\vec{B} = B_0 \hat{z}$ and being perturbed by an electrostatic wave, $\vec{E} = E_0 \hat{x} \sin(kx - \omega t)$, is given by

$$\frac{d^2 x}{dt^2} + \Omega^2 x = \frac{qE_0}{m} \sin(kx - \omega t) \quad (1)$$

where $\Omega = qB_0/m$ is the cyclotron angular frequency, and q and m are the charge and mass of the particle, respectively. We normalize time to Ω^{-1} and length to k^{-1} , and define the dimensionless variables $X = kx$ and $\tau = \Omega t$. The normalized action and angle (I, θ) of the linear oscillator (obtained from Eq. (1) by setting E_0 equal to 0) are such that $X = \rho \sin(\theta)$, $\dot{X} = \rho \cos(\theta)$, where $\dot{X} = dX/d\tau$, $\rho = \sqrt{2I}$ is the normalized Larmor radius, and $I = (X^2/2 + \dot{X}^2/2)$. In action-angle variables, the Hamiltonian corresponding to Eq. (1) is

$$H = I + \varepsilon \sum_{n=-\infty}^{\infty} J_n(\rho) \cos(n\theta - \nu\tau) \quad (2)$$

where $\varepsilon = (kqE_0)/(m\Omega^2)$, $\nu = \omega/\Omega$, and J_n is the Bessel function of order n .

We now focus on the case when ν is an integer. We show that the web structure, whose existence has only been derived for values of $\rho \geq \nu$, does not

extend down to $\rho = 0$. We then compute, both numerically and analytically, the last orbit deduced from (2) that does not connect to the web. This last orbit is referred to as the lower bound of the web (LWB).

The fact that the web has a lower bound can be easily understood directly from the equations of motion. A Hamilton equation deduced from (2) gives

$$\frac{d\rho}{d\tau} = \frac{\varepsilon}{\rho} \left[\nu J_\nu(\rho) \sin \nu(\theta - \tau) + \sum_{n \neq \nu} n J_n(\rho) \sin(n\theta - \nu\tau) \right]. \quad (3)$$

The first term on the RHS of (3) is at the origin of the existence of the web: keeping this term only in (3) yields the skeleton of the web structure⁵.

If $\nu > 1$, $J_\nu(\rho) \cos \nu(\theta - \tau)$ decreases faster than $\sum_{n \neq \nu} J_n(\rho) \cos(n\theta - \nu\tau)$ when $\rho \rightarrow 0$. Therefore, the term responsible for the web structure becomes negligible when $\rho \rightarrow 0$, which implies that the web does not extend down to $\rho = 0$.

An estimate of the lower bound of the web can be obtained by numerically solving the equations of motion deduced from the Hamiltonian (2). The value of the initial Larmor radius ρ_0 is gradually decreased until the LWB is found. Such a procedure is illustrated in Figures 1 and 2.

As expected, the numerical results indicate that the orbit forming the LWB is regular. Such an orbit can be obtained from an integrable Hamil-

tonian derived from (2) using perturbation theory. The procedure is similar to that used, for example, in proving the Kolmogorov Arnold Moser (KAM) theorem^{10,11}. In this letter, we derive the LWB using perturbation theory, but, unlike in the KAM theorem, we do a perturbation analysis only up to second order in ε . As will be shown, this leads to a very accurate description of the LWB. Thus, we do not aim to prove mathematically that for low enough initial values of the Larmor radius the variation of the action remains small for an infinite time but, rather, we explain analytically the numerical observations that the action remains nearly a constant for times very long compared to the cyclotron period (up to 10^6 cyclotron periods in the longest simulations).

The perturbation analysis is performed using the formalism of Lie transform¹². We follow the procedure detailed in Ref. 6, and introduce a generating Lie Hamiltonian χ , and define the transformation operator T , acting on any function g of the dynamical variables I and θ . T is such that $T\{g\}(I, \theta) = g(\tilde{I}, \tilde{\theta})$, where $(\tilde{I}, \tilde{\theta})$ is the position in phase space at “time” ε , of the trajectory defined by the Hamiltonian χ , with initial conditions (I, θ) . In particular, when g is the identity, this leads to the definition of the change of variables $(\tilde{I}, \tilde{\theta}) = T(I, \theta)$. This change of variables is clearly canonical. The time intro-

duced to define the transformation operator is a “fake” time for the auxiliary dynamics defined by χ , and is not related to the real time τ in (2).

In order to carry out a perturbation analysis, we expand, following Depri’s method¹³, χ in a power series in ε :

$$\chi = \sum_{i=0}^{+\infty} \varepsilon^i \chi_{i+1} . \quad (4)$$

The Hamiltonian (2) is already expanded in power series in ε : $H = H_0 + \varepsilon H_1$, where

$$H_0 = I \quad (5)$$

$$H_1 = \sum_{n=-\infty}^{\infty} J_n(\rho) \cos(n\theta - \nu\tau) . \quad (6)$$

In the new variables $(\tilde{I}, \tilde{\theta})$ the dynamics is given by a new Hamiltonian \tilde{H} that can also be expanded in power series in ε

$$\tilde{H} = \sum_{i=0}^{+\infty} \varepsilon^i \tilde{H}_i . \quad (7)$$

It is clear that $\tilde{H}_0 = H_0$ because when $\varepsilon = 0$, $(\tilde{I}, \tilde{\theta}) = (I, \theta)$.

Finally, we also expand the inverse transformation operator T^{-1} as a power series in ε ;

$$T^{-1} = \sum_{i=0}^{+\infty} \varepsilon^i T_i^{-1} \quad (8)$$

where T_0^{-1} is the identity since for $\varepsilon = 0$ $(\tilde{I}, \tilde{\theta}) = (I, \theta)$. For $i \geq 1$, it can be shown that T_i^{-1} is defined by the recursion relation

$$T_i^{-1} = \frac{1}{i} \sum_{j=0}^{i-1} L_{i-j} T_j^{-1} \quad (9)$$

where $L_i = \{\chi_i, \cdot\}$, and $\{\cdot, \cdot\}$ stands for the Poisson bracket.

One of the results of Deprit's method is the relation between the \tilde{H}_i 's, the H_i 's, the χ_i 's and the T_i^{-1} 's:

$$\frac{\partial \chi_i}{\partial \tau} + \{\chi_i, H_0\} = i(\tilde{H}_i - H_i) - \sum_{j=1}^{i-1} (L_{i-j} \tilde{H}_j + j T_{i-j}^{-1} H_j) . \quad (10)$$

This is a functional relation. In (10) H and \tilde{H} are functions of the same canonical variables. This is the main advantage of the Lie transform to not involve mixed variables. Using the definition (5) of H_0 , (10) becomes

$$\frac{\partial \chi_i}{\partial \tau} + \frac{\partial \chi_i}{\partial \theta} = i(\tilde{H}_i - H_i) - \sum_{j=1}^{i-1} (L_{i-j} \tilde{H}_j + j T_{i-j}^{-1} H_j) . \quad (11)$$

In (11), \tilde{H}_i is chosen so that no secularity appears in χ_i . Once \tilde{H}_i is thus specified, (11) is solved for χ_i .

At first order in perturbation theory ($i = 1$), (11) becomes

$$\frac{\partial \chi_1}{\partial \tau} + \frac{\partial \chi_1}{\partial \theta} = \tilde{H}_1 - \sum_{n=-\infty}^{\infty} J_n(\rho) \cos(n\theta - \tau) . \quad (12)$$

The only term that leads to secularities in χ_1 is $J_\nu(\rho) \cos \nu(\theta - \tau)$. Thus, we choose $\tilde{H}_1 = J_\nu(\tilde{\rho}) \cos \nu(\tilde{\theta} - \tau)$. Then, the contribution of the first order to

the generating Lie Hamiltonian is

$$\chi_1 = \sum_{m \neq \nu} \frac{J_m(\tilde{\rho}) \cos(m\tilde{\theta} - \nu\tau)}{m - \nu} . \quad (13)$$

To first order, the transformed Hamiltonian is

$$\tilde{H} = \tilde{I} + \varepsilon J_\nu(\tilde{\rho}) \cos \nu(\tilde{\theta} - \tau) . \quad (14)$$

We then define a canonical change of variables $(\tilde{I}, \tilde{\theta}) \mapsto (\tilde{J}, \tilde{\Phi})$ using the generating function

$$F = \tilde{J}(\tilde{\theta} - \tau) \quad (15)$$

which yields $\tilde{J} = \tilde{I}$, and $\tilde{\Phi} = \tilde{\theta} - \tau$. In variables $(\tilde{J}, \tilde{\Phi})$, (14) becomes

$$\tilde{H} = \varepsilon J_\nu(\tilde{\rho}) \cos(\nu\tilde{\Phi}) . \quad (16)$$

The orbits of Hamiltonian (16) are obtained by solving $\tilde{H} = \text{const.}$ Hence stopping at first order in perturbation theory yields nothing but the web structure. Therefore, in order to find the LWB, we have to go at least to the second order in perturbation theory.

To second order, (11) gives

$$\frac{\partial \chi_2}{\partial \tau} + \frac{\partial \chi_2}{\partial \theta} = 2(\tilde{H}_2 - H_2) - L_1(\tilde{H}_1 + H_1) . \quad (17)$$

Following the calculations in ⁶ we can show that, in order to avoid secularities in χ_2 , we have to choose

$$\tilde{H}_2 = S_1(\tilde{\rho}) + \cos 2\nu(\tilde{\theta} - \tau) S_2(\tilde{\rho}) \quad (18)$$

where

$$S_1(\tilde{\rho}) = \sum_{m \neq \nu} \frac{m}{2\tilde{\rho}(\nu - m)} J_m(\tilde{\rho}) J'_m(\tilde{\rho}) \quad (19)$$

$$S_2(\tilde{\rho}) = \sum_{m \neq \nu} \frac{m}{2\tilde{\rho}(\nu - m)} J_m(\tilde{\rho}) J'_{2\nu-m}(\tilde{\rho}) \quad (20)$$

and the prime denotes the derivative with respect to $\tilde{\rho}$. The sums S_1 and S_2 can be carried out analytically. As shown in Ref. 6, when x is not an integer

$$\begin{aligned} \bar{S}_1(\tilde{\rho}) &= \sum_{m=-\infty}^{\infty} \frac{m}{2\tilde{\rho}(x - m)} J_m(\tilde{\rho}) J'_m(\tilde{\rho}) \\ &= \frac{\pi}{8 \sin(x\pi)} [J_{x+1}(\tilde{\rho}) J_{-x-1}(\tilde{\rho}) - J_{x-1}(\tilde{\rho}) J_{-x+1}(\tilde{\rho})] \end{aligned} \quad (21)$$

$$\begin{aligned} \bar{S}_2(\tilde{\rho}) &= \sum_{m=-\infty}^{\infty} \frac{m}{2\tilde{\rho}(x - m)} J_m(\tilde{\rho}) J'_{2x-m}(\tilde{\rho}) \\ &= \frac{\pi}{16} \cot(\pi x) (J_{x-1}^2 - J_{x+1}^2) + \frac{1}{8\tilde{\rho}^2} \int_0^{2\tilde{\rho}} \rho J_{2x}(\rho) d\rho. \end{aligned} \quad (22)$$

From (19) and (21):

$$\begin{aligned} S_1 &= \lim_{x \rightarrow \nu} \left[\bar{S}_1(\tilde{\rho}) - \frac{\nu J_\nu(\tilde{\rho}) J'_\nu(\tilde{\rho})}{2\tilde{\rho}(x - \nu)} \right] \\ &= \frac{(-1)^\nu}{8} J_{\nu+1} \left[\left(\frac{\partial J_{-x-1}}{\partial x} \right)_{x=\nu} + (-1)^{\nu+1} \left(\frac{\partial J_{1+x}}{\partial x} \right)_{x=\nu} \right] \\ &\quad + \frac{(-1)^{\nu+1}}{8} J_{\nu-1} \left[\left(\frac{\partial J_{-x+1}}{\partial x} \right)_{x=\nu} + (-1)^{\nu+1} \left(\frac{\partial J_{-1+x}}{\partial x} \right)_{x=\nu} \right]. \end{aligned} \quad (23)$$

Using (20) and (22) we find

$$\begin{aligned}
S_2 &= \lim_{x \rightarrow \nu} \left[\bar{S}_2(\tilde{\rho}) - \frac{\nu J_\nu(\tilde{\rho}) J'_{2x-\nu}(\tilde{\rho})}{2\tilde{\rho}(x-\nu)} \right] \\
&= \frac{1}{8} \left[J_{\nu-1} \left(\frac{\partial J_{x-1}}{\partial x} \right)_{x=\nu} - J_{\nu+1} \left(\frac{\partial J_{x+1}}{\partial x} \right)_{x=\nu} + \frac{1}{\tilde{\rho}^2} \int_0^{2\tilde{\rho}} \rho J_{2\nu}(\rho) d\rho \right] \\
&\quad - \frac{\nu}{4\tilde{\rho}} J_\nu \left[\left(\frac{\partial J_{x-1}}{\partial x} \right)_{x=\nu} - \left(\frac{\partial J_{x+1}}{\partial x} \right)_{x=\nu} \right]. \tag{24}
\end{aligned}$$

Numerical calculations show that, when $\tilde{\rho} < \nu$

$$S_2(\tilde{\rho}) \ll S_1(\tilde{\rho}). \tag{25}$$

Also, for $\tilde{\rho} < \nu$, $(\partial J_x / \partial x)_{x=\nu} \ll (\partial J_{-x} / \partial x)_{x=\nu}$. Using the definition of the Weber's function $Y_\nu = (1/\pi)[(\partial J_x / \partial x)_{x=\nu} - (-1)^\nu (\partial J_{-x} / \partial x)_{x=\nu}]$, for $\tilde{\rho} < \nu$ (23) gives:

$$S_1(\tilde{\rho}) \simeq \pi/8 [J_{\nu+1}(\tilde{\rho}) Y_{\nu+1}(\tilde{\rho}) - J_{\nu-1}(\tilde{\rho}) Y_{\nu-1}(\tilde{\rho})]. \tag{26}$$

Finally, by transforming to the variables $(\tilde{J}, \tilde{\Phi})$ defined by the generating function (15), the transformed Hamiltonian up to second order in perturbation theory is

$$\tilde{H} = \varepsilon J_\nu(\tilde{\rho}) \cos(\nu \tilde{\Phi}) + \pi \varepsilon^2 / 8 [J_{\nu+1}(\tilde{\rho}) Y_{\nu+1}(\tilde{\rho}) - J_{\nu-1}(\tilde{\rho}) Y_{\nu-1}(\tilde{\rho})]. \tag{27}$$

The original variables (I, θ) can be expressed in terms of $(\tilde{I}, \tilde{\theta})$ by computing

the inverse Lie transform to first order:

$$I = \tilde{I} + \frac{\partial \chi_1}{\partial \tilde{\theta}} = \tilde{I} + \varepsilon \sum_{m \neq \nu} \frac{m J_m(\tilde{\rho}) \cos(m\tilde{\theta} - \nu\tau)}{\nu - m} \quad (28)$$

$$\theta = \tilde{\theta} - \frac{\partial \chi_1}{\partial \tilde{I}} = \tilde{\theta} - \frac{\varepsilon}{\tilde{\rho}} \sum_{m \neq \nu} \frac{J'_m(\tilde{\rho}) \sin(m\tilde{\theta} - \nu\tau)}{\nu - m}. \quad (29)$$

Note that in order to obtain the transformed Hamiltonian \tilde{H} we kept the perturbation analysis up to second order, while for the calculation of the inverse Lie transform we only used the results to first order. This is due to the fact that at first order \tilde{H} contains only the term $J_\nu(\tilde{\rho})$ which decreases, for $\nu \geq 1$, faster than the terms of the second order when $\tilde{\rho} \rightarrow 0$. This effect does not exist in the calculation of the inverse Lie transform as χ_1 already contains Bessel functions of low order.

To second order in perturbation theory, the orbits are obtained by solving $\tilde{H} = \text{const}$. This leads to a curve in the variables $(\tilde{I}, \tilde{\Phi} = \tilde{\theta} - \tau)$. If we restrict the values of $\tilde{\Phi}$ and $\tilde{\theta}$ to be between 0 and 2π , and if $\tau = 0 \bmod 2\pi$ like for a Poincaré section at $\tau = 0$ for example, then $\tilde{\Phi} = \tilde{\theta}$.

Solving $\tilde{H} = \text{const}$ for parameters corresponding to Figure 2, and going back to the original variables using (28) and (29), with $\tau = 0$, leads to the curve plotted in Figure 3. This curve is very close to the Poincaré section obtained numerically from the full Hamiltonian (2), and shown in Figure 2.

This shows the accuracy of the second order perturbation theory.

Using (27) we can compute the lower bound of the web. Solving $\tilde{H} = \text{const}$, where the constant corresponds to the initial condition $\tilde{I}(0) = \tilde{I}_0$ and $\tilde{\theta}(0) = \pi/2\nu$, leads to the equation

$$\cos(\nu\tilde{\Phi}) = \varepsilon \frac{S_1(\tilde{\rho}_0) - S_1(\tilde{\rho})}{J_\nu(\tilde{\rho})} \quad (30)$$

$f_\nu(\tilde{\rho}, \tilde{\rho}_0) \equiv | [S_1(\tilde{\rho}_0) - S_1(\tilde{\rho})] / J_\nu(\tilde{\rho}) |$ is continuous in $[\tilde{\rho}_0, \nu]$ and therefore has a maximum, f_m , in this interval. Now, because of (30), if $f_m > 1$ then $\tilde{\rho}$ is bounded, namely $\tilde{\rho} \leq \tilde{\rho}_m$, where ρ_m is the lowest value of $\tilde{\rho}$ in $[\tilde{\rho}_0, \nu]$ such that $f_\nu(\tilde{\rho}_m, \tilde{\rho}_0) = 1$. If $f_m \leq 1$, the value $\tilde{\rho} = \nu$ can be reached. As it is known that the web structure exists in the region of phase space corresponding to $\tilde{\rho} \geq \nu$, it follows that when $f_m \leq 1$ a particle accesses the web and its dynamics is chaotic. Thus, we have a very precise analytic criterion for determining the lower bound of the web. We can determine numerically, with great precision, the value of $\tilde{\rho}_0$ such that $f_m \simeq 1$. This allows us to find a very good estimate of the LWB. We then compute, for the orbit corresponding to our approximate solution of the LWB, the average, $\langle \rho \rangle_\theta$, of the Larmor radius ρ , over the angle θ . Figure 4 plots $\langle \rho \rangle_\theta$ versus ε for $\nu = 5$. The results obtained using perturbation theory up to second

order are in very good agreement with the estimates of the LWB obtained by numerically integrating the equations of motion deduced from Hamiltonian (2), as in the case of Figs. 1 and 2.

The striking feature of Fig. 4 is that $\langle \rho \rangle_\theta$ is an increasing function of ε . This implies, for example, that a particle with an initial Larmor radius close to 0.6 will not access the web if $\varepsilon > 0.3$. However, its dynamics will be stochastic for values of ε less than 0.3. Thus, a particle's dynamics can be made stochastic by decreasing the amplitude of the wave!

The lifting of the LWB to higher energies with ε is more sensitive for low values of ν . This can be seen by making a small $\tilde{\rho}$ expansion of $f_\nu(\tilde{\rho}, \tilde{\rho}_0)$, which gives a good approximation of f_ν as long as $\tilde{\rho} < \nu$. To lowest order in $\tilde{\rho}$, and for $\nu > 2$, (30) becomes

$$\cos(\nu\tilde{\Phi}) = \varepsilon \frac{3 \times 2^{\nu-3} \nu(\nu-3)!}{(\nu+2)(\nu+1)} \left(\frac{\tilde{\rho}^2 - \tilde{\rho}_0^2}{\tilde{\rho}^\nu} \right). \quad (31)$$

The approximate position of the minimum of $f_\nu(\tilde{\rho}, \tilde{\rho}_0)$, as given by the small $\tilde{\rho}$ expansion, is at $\tilde{\rho}^* \simeq \sqrt{[\nu/(\nu+2)]} \tilde{\rho}_0$. The value of $\tilde{\rho}_0$ corresponding to the LWB is such that $f_\nu(\tilde{\rho}^*, \tilde{\rho}_0) = 1$, which, according to (31), leads $\tilde{\rho}_0$ to scale as $\varepsilon^{1/(\nu-2)}$. Therefore, $\tilde{\rho}_0$ is less sensitive to the value of ε when ν increases. Figure 5 plots $\langle \rho \rangle_\theta$ versus ε for $\nu = 140$. It is clear that $\langle \rho \rangle_\theta$ varies much less

as a function of ε than for the case $\nu = 5$.

The method used to compute the LWB is only valid for small values of ε . Indeed, using a trapping idea, Karney and Bers¹ have shown that a particle's dynamics is stochastic when its Larmor radius is such that $\rho > \nu - \sqrt{\varepsilon}$. Thus the perturbation theory breaks down when the LWB is for values of ρ larger than $\nu - \sqrt{\varepsilon}$. For large values of ε the lower bound of the stochastic region decreases with ε . This effect is illustrated in Fig. 5.

In conclusion, we have studied the interaction of a charged particle with an electrostatic wave propagating perpendicularly to a uniform magnetic field, for the case when the wave frequency is an integer multiple of the particle cyclotron frequency. We have shown that the web structure, which exists only in this on-resonance case, has a lower bound and does not extend to $\rho = 0$. For values of the wave amplitude such that the LWB is for ρ lower than $\nu - \sqrt{\varepsilon}$, we have obtained an accurate description of the LWB by using Lie perturbation theory up to second order. We find that the LWB moves to higher energies as the amplitude of the wave is increased. This implies that the dynamics of particles with low energies can be made chaotic as the wave amplitude is decreased.

Acknowledgments

D.B. acknowledges the hospitality of the Plasma Science and Fusion Center during the course of this research. D.B. was supported by a Lavoisier grant from the French Ministère des Affaires Etrangères. A.K.R. and A.B. are supported by NSF Grant Number ATM-94-24282 and DoE Grant DE-FG02-91ER-54109.

REFERENCES

- ¹ C. F. F. Karney and A. Bers, *Phys. Rev. Lett.*, **39**, 550 (1977).
- ² C. F. F. Karney, *Phys. Fluids*, **21**, 1584 (1978).
- ³ C. F. F. Karney, *Phys. Fluids*, **22**, 2188 (1979).
- ⁴ A. Fukuyama, H. Momota, R. I. Tatani, and T. Takizuka, *Phys. Rev. Lett.*, **38**, 701 (1977).
- ⁵ G. M. Zaslavsky, R. Z. Sagdeev, D. A. Usikov, and A. A. Chernikov, *Weak Chaos and Quasi-Regular Patterns* (Cambridge University Press, 1991).
- ⁶ Ping-Kun Chia, L. Schmitz, and R. W. Conn, *Phys. Plasmas*, **3**, 1545 (1996).
- ⁷ A. J. Lichtenberg and M. A. Lieberman, *Regular and Chaotic Dynamics*, 2nd ed. (Springer Verlag, New York, 1992).
- ⁸ H. Pacher, C. Gormezano, W. Hess, G. Ichtchenko, R. Magne, T.-K. Nguyen, G. W. Pacher, F. Söldner, G. Tonon, and J.-G. Wegrowe, in *Heating in Toroidal Plasmas*, Proceedings of the 2nd Joint Grenoble-Varenna International Symposium, Como, Italy, September 3–12, 1980, eds. E. Canobbio, H. P. Eubank, G. G. Leotta, A. Malein, and E. Sindoni (1980), p. 329.
- ⁹ J. L. Vago, P. M. Kintner, S. Chesney, R. L. Arnoldy, K. A. Lynch, T. E.

Moore, and C. J. Pollock, *J. Geophys. Res.*, **97**, 16935 (1992).

¹⁰ A. N. Kolmogorov, *Dok. Akad. Nauk. SSSR*, **98**, 527, (1954). English translation in *Stochastic Behavior in Classical and Quantum Hamiltonian Systems*, eds. G. Casati and J. Ford (Springer Verlag, New York, 1979).

¹¹ G. Benettin, L. Galgani, A. Giorgilli, and J. M. Strelcyn, *Il Nuovo Cimento*, **79**, 201 (1984).

¹² J. Cary, *Phys. Rep.*, **79**, 129 (1981).

¹³ A. Deprit, *Celest. Mech.*, **1**, 12 (1969).

Figure Captions

Figure 1: Poincaré section at time $\tau = 0 \bmod 2\pi$ of the dynamics defined by the Hamiltonian (2), with initial conditions $\rho_0 = 0.82$, $\theta_0 = 0$. Such an initial condition leads a particle to access the web.

Figure 2: Poincaré section at time $\tau = 0 \bmod 2\pi$ of the dynamics defined by the Hamiltonian (2) with initial conditions $\rho_0 = 0.81$, $\theta_0 = 0$. For this initial condition a particle does not access the web. As this initial condition is very close to the one of Figure 1, this curve is a good numerical estimate of the LWB.

Figure 3: Orbit obtained by solving $\tilde{H} = \text{const}$, using (27), where the constant is chosen to correspond to the same parameters as in Figure 2.

Figure 4: $\langle \rho \rangle_\theta$ calculated on the lower bound of the web as a function of ε for $\nu = 5$. The solid line is obtained from the second order perturbation theory, while the pluses are the numerical estimates obtained as in the case of Figure 1 and Figure 2.

Figure 5: $\langle \rho \rangle_\theta$ calculated on the lower bound of the web as a function of ε for $\nu = 140$. The solid line corresponds to the results obtained using perturbation theory kept up to second order and the pluses are the numerical estimates. The dashed line is the lower bound of the chaotic region obtained by using the trapping idea of Ref. 1.

FIG. 1

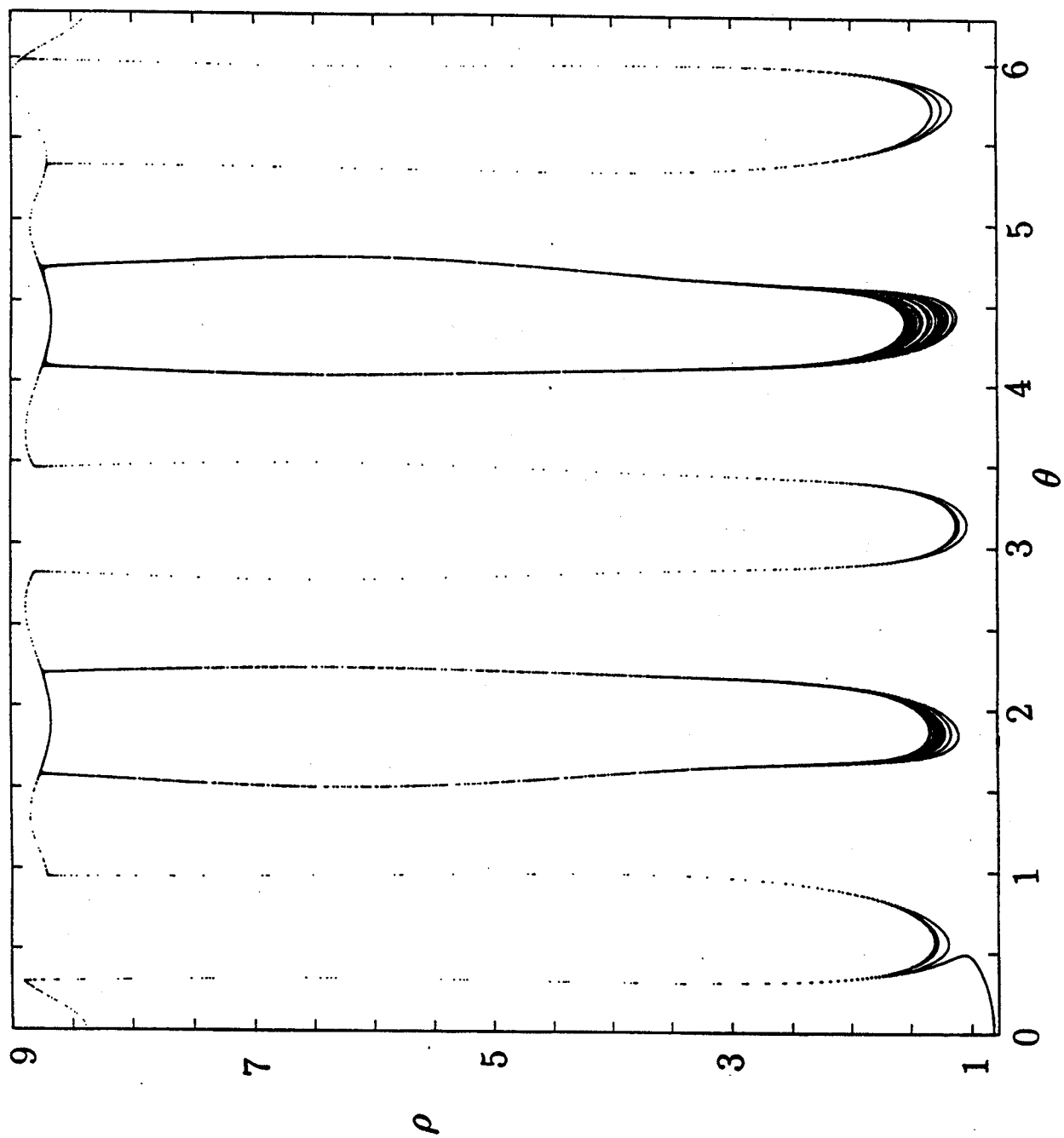


FIG. 2

